ISME

www.nature.com/ismej

ARTICLE

Molecular mechanisms underlying iron and phosphorus co-limitation responses in the nitrogen-fixing cyanobacterium *Crocosphaera*

Nina Yang[1], Yu-An Lin[1], Carlin A. Merkel[1], Michelle A. DeMers[1], Ping-Ping Qu[1,2], Eric A. Webb[1], Fei-Xue Fu[1] and David A. Hutchins[1]✉

In the nitrogen-limited subtropical gyres, diazotrophic cyanobacteria, including *Crocosphaera*, provide an essential ecosystem service by converting dinitrogen (N_2) gas into ammonia to support primary production in these oligotrophic regimes. Natural gradients of phosphorus (P) and iron (Fe) availability in the low-latitude oceans constrain the biogeography and activity of diazotrophs with important implications for marine biogeochemical cycling. Much remains unknown regarding *Crocosphaera*'s physiological and molecular responses to multiple nutrient limitations. We cultured *C. watsonii* under Fe, P, and Fe/P (co)-limiting scenarios to link cellular physiology with diel gene expression and observed unique physiological and transcriptional profiles for each treatment. Counterintuitively, reduced growth and N_2 fixation resource use efficiencies (RUEs) for Fe or P under P limitation were alleviated under Fe/P co-limitation. Differential gene expression analyses show that Fe/P co-limited cells employ the same responses as single-nutrient limited cells that reduce cellular nutrient requirements and increase responsiveness to environmental change including smaller cell size, protein turnover (Fe-limited), and upregulation of environmental sense-and-respond systems (P-limited). Combined, these mechanisms enhance growth and RUEs in Fe/P co-limited cells. These findings are important to our understanding of nutrient controls on N_2 fixation and the implications for primary productivity and microbial dynamics in a changing ocean.

The ISME Journal; https://doi.org/10.1038/s41396-022-01307-7

INTRODUCTION

The availability of the biologically essential macronutrients nitrogen (N) and phosphorus (P), and micronutrients like iron (Fe), plays a critical role in the productivity and distribution of phytoplankton communities in the ocean [1, 2]. In the nutrient-poor or oligotrophic open ocean ecosystems where N scarcity generally limits phytoplankton growth [1], a group of specialized cyanobacteria carry out nitrogen fixation (N_2 fixation), converting dinitrogen (N_2) gas into a more biologically accessible form of N, ammonia [3, 4]. This input of "new" N by cyanobacterial N_2 fixers or diazotrophs, including the filamentous, colony-forming *Trichodesmium* and unicellular diazotrophs (e.g., the obligate symbiont UCYN-A, and free-living *Crocosphaera*), supports a significant portion of primary production in the subtropical and tropical oligotrophic waters [3, 5–7]. While *Trichodesmium* has been intensely studied for decades as a primary contributor to marine N_2 fixation [8–12], the ecological and biogeochemical relevance of unicellular diazotrophs, including *Crocosphaera*, has only been recognized more recently [13–18].

Despite our growing recognition of *Crocosphaera*'s importance in oligotrophic systems, we still have limited understanding of how the availability of nutrients, especially P and Fe, constrain their biogeography and activity [19–21]. P is an essential component of various cellular molecules including membranes, ribosomes, nucleic acids, and the energy source, adenosine triphosphate (ATP) [22]. It is also crucial in two-component regulatory systems that enable the cell to sense and respond to environmental changes [23, 24]. Fe is an essential micronutrient for phytoplankton, serving as a cofactor of numerous metabolic processes including photosynthesis, chlorophyll biosynthesis, and respiratory electron transport [25]. In addition, N_2 fixers including *Crocosphaera* have a much higher cellular Fe demand than non-diazotrophic phytoplankton because the nitrogenase metalloenzyme that facilitates N_2 fixation is an Fe-rich enzyme complex [26, 27]. Thus, in oligotrophic ecosystems, the availability of P and Fe may impact core diazotrophic cellular processes and metabolisms that play a key role in marine biogeochemical cycling.

Previous studies have suggested that the distributions of N_2 fixers and N_2 fixation rates in the subtropical and tropical open oceans are shaped and constrained by the relative availability of P and Fe across different oceanic basins [3, 4, 28]. For example, the North Atlantic Subtropical Gyre, which receives Fe via episodic inputs of eolian dust from the Sahara Desert, is relatively more P-limited than the North Pacific Subtropical Gyre, where a lack of aeolian Fe input yields a more Fe-limited system [1, 4, 29].

[1]Department of Biological Sciences, University of Southern California, Los Angeles, CA, USA. [2]Present address: Department of Psychiatry and Behavioral Sciences, Stanford University School of Medicine, Stanford, CA, USA. ✉email: dahutch@usc.edu

Received: 27 February 2022 Revised: 4 August 2022 Accepted: 9 August 2022
Published online: 25 August 2022

Under low P or Fe conditions, N_2 fixers have evolved various strategies to acquire and conserve these elements efficiently. These nutrient acquisition systems have been applied as Fe and/or P limitation indicators. Under P limitation, these strategies include a mechanism for high-affinity phosphate transport via the upregulation of the phosphate-binding gene, *pstS* [10, 30, 31]. Another mitigating response is the use of dissolved organic phosphorus (e.g., phosphomonoesters), indicated by upregulation of the alkaline phosphatase (*phoA/B, phoX*) genes [10, 30, 32, 33].

When Fe-limited, cells downregulate gene expression of Fe-rich Photosystem I (PSI) protein complexes while upregulating the expression of an Fe stress-induced chlorophyll-binding gene, *isiA* [34, 35]. IsiA proteins form Fe-free light-harvesting antennae that shield the photosynthetic apparatus from oxidative damage [15, 36]. In addition, cyanobacterial diazotrophs can substitute the Fe-containing electron transfer protein ferredoxin with the Fe-free flavodoxin, IsiB [37, 38]. Unlike *Trichodesmium*, which simultaneously photosynthesize and fix N_2 during the day, *Crocosphaera* temporally separates these two processes and fixes N_2 at night [39]. This unicellular diazotroph has evolved the ability to shuttle cellular Fe between Fe-containing proteins in the photosynthetic apparatus and those in the nitrogenase complex through diel synthesis and degradation of these core metalloenzymes [40]. This Fe conservation strategy substantially reduces *Crocosphaera*'s cellular Fe requirements that may better enable *Crocosphaera* to inhabit Fe-depleted waters compared to *Trichodesmium* [40].

Recent lab and field studies have found that N_2 fixers may be well-adapted to environments that are low in both P and Fe, or Fe/P co-limited [41–43]. Fe/P co-limitation can produce unexpected physiological responses, including enhanced growth and N_2 fixation rates, and cell size reductions compared to either P or Fe single-nutrient limitation responses [21, 42–44]. Most of these studies focus on the molecular mechanisms underlying the Fe/P co-limited response in *Trichodesmium*, which include a shift in protein abundance patterns unique to the Fe/P co-limited response in various metabolic pathways linked to cell size reduction and increased growth rates [44].

To our knowledge, only one study has been conducted on the Fe/P co-limited physiological response in *Crocosphaera*, while the molecular response mechanisms involved remain uncharacterized [21]. To study the molecular response, we grew one *Crocosphaera watsonii* isolate under Fe, P, and Fe/P (co)-limiting conditions and conducted differential gene expression analyses to link physiology with the underlying mechanisms of nutrient-limited responses and their implications for marine nitrogen biogeochemistry.

METHODS

Culturing methods

Triplicate cultures of *C. watsonii* strain WH0005 were grown at 28 °C in microwave-sterilized Aquil medium made with 0.2 µm-filtered artificial seawater (ASW) [45]. The seawater base was amended with Fe buffered with 25 µM EDTA, P, vitamins, and trace metals [46]. In an approach modified from Walworth et al., cultures were maintained semi-continuously under Fe/P co-limitation for ~3 months and single-nutrient and replete treatments were generated by adding back Fe (P-limited), P (Fe-limited), and Fe + P (Replete) followed by an additional 1.5 months of growth before sampling [44]. Culture maintenance followed previously described trace metal-clean methods [46]. Prior to sampling, cultures were grown for two weeks (~3–7 generations) in ASW passed through an activated Chelex 100 resin column (BioRad Laboratories, Hercules, CA, USA) to remove contaminating Fe followed by nutrient amendments described above. The entire media recipe with nutrient amendments is detailed in the Supplementary Methods.

Physiological measurements

Previously published methods were used for physiological measurements [46–48] and are detailed further in the Supplementary Methods. Briefly, cell counts were used to calculate specific growth rates (μ) using the equation $\mu = (\ln N_1 - \ln N_0)/t$, where N refers to cell densities and t is time in days. Cell size was determined by measuring cell diameters of 65 cells per sample at 400× magnification using the CaptaVision Imaging Software (Commack, NY, USA).

Net primary productivity or carbon fixation (C fixation) was assessed using the radiocarbon labeled bicarbonate ($H^{14}CO_3$) method. Sub-cultures (10 mL) were incubated for 6 hours with $H^{14}CO_3$, filtered onto glass microfiber filters (Whatman, Grade GF/F), stored in the dark overnight, and subsequently analyzed on a Beckman LS 6000 liquid scintillation counter (Beckman Coulter Inc., Fullerton, CA, USA). N_2 fixation was measured using the acetylene reduction assay. Sub-cultures (40 mL) from each replicate were injected with 6 mL of acetylene (~17% of headspace) at the start of the dark period. All-night (~12 h) accumulation of ethylene was measured on a GC-8A gas chromatograph (Shimadzu Scientific Instruments, Columbia, Maryland) and converted to fixed N_2 using a ratio of 3:1 and a Bunsen coefficient of 0.086. Measured C fixation and N_2 fixation rates were then normalized to daytime and nighttime cell counts, respectively.

Resource Use Efficiencies (RUEs) were calculated by normalizing measured C fixation and N_2 fixation rates to cellular P (C-PUEs, N-PUEs, mol C or N fixed h^{-1} mol cellular P^{-1}) or to cellular Fe content (C-IUEs, and N-IUEs, mol C or N fixed h^{-1} mol cellular Fe^{-1}) [46, 49]. Cellular C, N, P, and Fe samples to calculate RUEs and elemental ratios were obtained following previously published methods [46, 48, 50] (see Supplementary Methods).

Statistical analyses

Statistical significance for physiological measurements and RUEs were calculated for all four nutrient treatments and for nutrient-limited treatments by one-way ANOVA with Tukey's HSD post-hoc analysis (p value < 0.05) using R v4.1.1. Welch's t test was conducted for pairwise comparisons of two treatments (p value < 0.05). The cellular Fe value of one Fe-limited replicate was removed from analyses due to likely contamination during sample collection, and IUEs and elemental ratios were calculated with the mean cellular Fe value of the remaining two replicates (see Supplementary Methods).

RNA extractions and sequencing

Sub-cultures (400 mL, ~7-8 × 10^7 cells) were collected 5-6 h into the light period and 5-6 h after dark (24 samples total) via centrifugation (Supplementary Methods). The pellets were transferred to cryogenic vials, flash frozen, and stored in liquid N_2 until extraction.

RNA was extracted using guanidium thiocyanate-phenol-chloroform (TRI Reagent, Sigma Aldrich) and Zymo's Direct-zol RNA Miniprep kit (Zymo Research, Irvine, CA) with a DNase treatment following kit instructions. RNA purity was checked using a Nanodrop spectrophotometer (Thermo Scientific) and sent to UC Davis' DNA Technologies Core for library preparation, and 150-bp paired-end sequencing on a NovaSeq S4 (Illumina).

Raw paired-end reads were quality checked using FastQC [51] and trimmed using Trimmomatic v0.39 in paired-end mode with the following settings to remove adapters: TRAILING:10 SLIDINGWINDOW:5:20 MINLEN:36 [52]. Trimmed sequences were mapped onto a new low-contig *Crocosphaera* WH0005 genome annotated with KofamScan [53] using end-to-end alignment mode in Bowtie2 v2.4.2 [54]. Alignments were converted to BAM files, sorted by read name, and filtered by mapping quality score (MAPQ) of 10 or higher using SAMtools v1.11 [55]. Sequences were tabulated using featureCounts from the Subread package v2.0.1 in stranded mode [56].

Transcriptomic analysis and visualizations

Gene counts were assigned Kyoto Encyclopedia of Genes and Genomes database (KEGG) Orthology identifiers (KO) from the KofamScan-annotated genome [57]. The *isiA* gene was identified by a nucleotide BLAST querying known *isiA* sequences from a previous *Crocosphaera* WH0005 genome [15] and the reference genome. The *isiA* and *isiB* (flavodoxin) genes are often polycistronic [15, 58] and as expected, both were on the same contig in our reference genome. KO-annotated and *isiA* read counts were summed to remove duplicate gene identifiers. Then, genes with low counts were removed if the mean for all treatments was less than five, yielding 3770 "unique genes".

All transcriptomic analyses and visualizations were performed in R v4.1.1. Differential gene expression (DGE) was conducted with DESeq2 v1.32.0, which uses a negative binomial generalized linear model to assess DGE for a design formula [43, 59]. Pairwise comparisons for day and night samples for each nutrient treatment (diel genes) and for nutrient-limited treatments

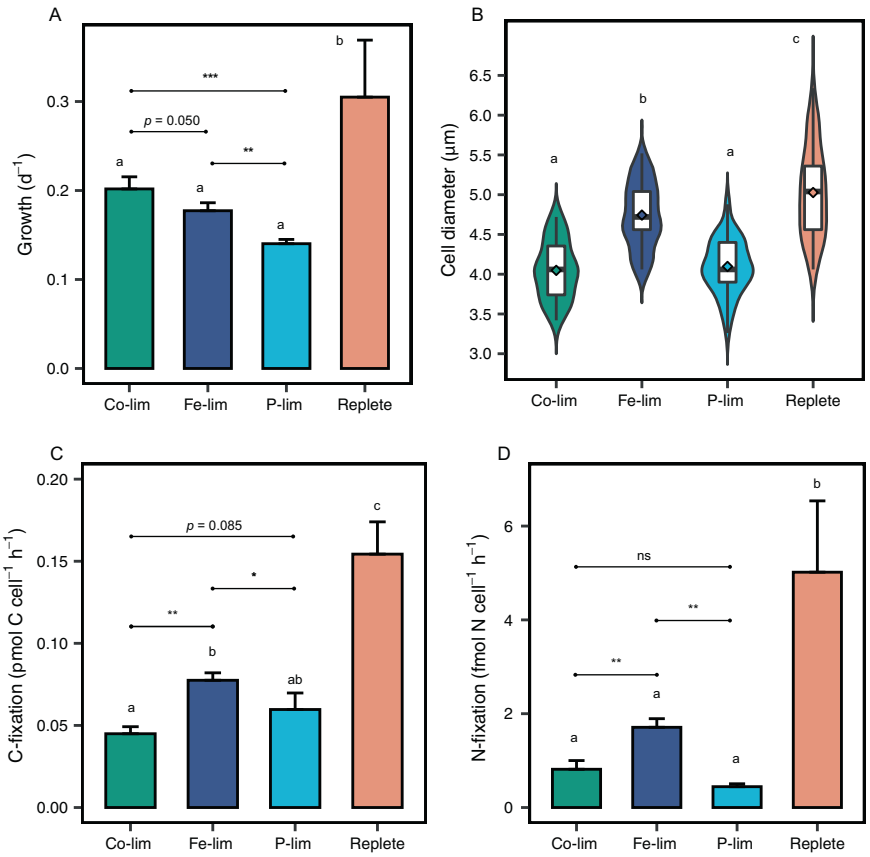

Fig. 1 Nutrient replete and nutrient-limited *Crocosphaera* physiology. A growth rates, **B** cell diameter, **C** carbon fixation (C fixation), and **D** nitrogen fixation (N_2 fixation) rates. For **B** a violin plot shows the distribution of the cell diameter datapoints, while the embedded diamond marker in the boxplot marks the mean cell diameter. Error bars denote standard deviation of triplicate values. Different letters on each plot represent statistical significance ($p < 0.05$) calculated by one-way ANOVA across all four treatments. Line segments and corresponding significance markers represent statistical significance calculated by one-way ANOVA across only the nutrient-limited treatments. Plots without line segments indicate that one-way ANOVA results with nutrient-limited only treatments were the same as results calculated with all treatments. Co-lim (Fe/P co-limited, green), Fe-lim (Fe-limited, dark blue), P-lim (P-limited, light blue), and Replete (Fe/P replete, peach). Significance: *($p < 0.05$), **($p < 0.01$), ***($p < 0.001$).

relative to the replete treatment were assessed by the default Wald test in DESeq2 with Benjamin-Hochberg (BH) adjusted p value < 0.05).

Over-representation analysis of differentially expressed genes (DEGs) was conducted using enrichKEGG (KEGG) and enricher (Gene Ontology, GO) functions from clusterProfiler v4.0.5, which calculates overrepresented or "enriched" biological pathways and functions using a hypergeometric test with a BH-adjusted p value < 0.05 [60]. For GO enrichment, the genome was annotated following published methods using DIAMOND (blastx mode, more-sensitive) against the NCBI nr database downloaded on August 31, 2021 (median E-value = 2.66×10^{-75}, median bitscore = 235), adding an additional 110 annotations to the 4502 KEGG-annotated reads (Supplementary Table S1). The DIAMOND output was then used for GO annotation by Blast2GO, InterProScan, and UniProt [61–64].

Gene counts were "regularized log" transformed using the rlog function (DESeq2) for redundancy analysis (RDA) using the rda function from the vegan v2.5-7 package [65]. Gene counts normalized using the median of ratios method (DESeq2) were used for boxplot and heatmap visualizations. Venn diagrams and heatmaps were generated using VennDiagram v1.6.20 and ComplexHeatmap v2.8.0 packages, respectively. Heatmap Z-scores were calculated for each gene by subtracting the gene expression from the row mean and then divided by the row standard deviation. All other graphs were generated using ggplot2 v3.3.5.

RESULTS AND DISCUSSION

Crocosphaera physiology and function under different nutrient conditions

We measured physiological parameters for *Crocosphaera* grown under different Fe and P limitation scenarios to compare and contrast their response to single-nutrient (Fe or P) and dual-nutrient (Fe/P) (co)-limitation (hereafter, co-limited or co-limitation). We define co-limitation as *Crocosphaera*'s growth response to simultaneous low Fe and P concentrations, either of which would be growth-limiting alone. In our study, the limiting concentrations of Fe and P for the co-limiting treatment were the same as those used in the single Fe- or P-limited conditions. All three nutrient-limited conditions were compared to the replete condition for a baseline comparison. As expected, all nutrient-limited *Crocosphaera* growth rates were less than replete rates (Fig. 1A). Co-limited *Crocosphaera* had the fastest growth rates of the nutrient-limited treatments, growing 14% faster than Fe-limited cells ($p = 0.050$) and ~44% faster than P-limited cells ($p < 0.001$). P-limited cells had the slowest growth.

On average, nutrient-limited cells were also smaller than replete cells, with mean cell diameters <5 µm for limited cells and >5 µm for the replete cells (Fig. 1B, $p < 0.001$). Co-limited and P-limited cells were similar in size with mean cell diameters of 4.05 µm and 4.1 µm, respectively. Fe-limited cells had a mean diameter of 4.7 µm. A smaller cell size increases the surface area-to-volume ratio and enables better access to nutrients than larger cells while also reducing the cellular requirements for limiting nutrients like Fe and P [21, 66]. Previous studies showed similar size changes under co-limited and Fe-limited conditions [20, 21] but did not report a decrease in size for P-limited cells [21]. Both Garcia et al. [20] and our study used a large-cell *Crocosphaera* phenotype (WH0005 and WH0003, respectively) with similar genomic capacity

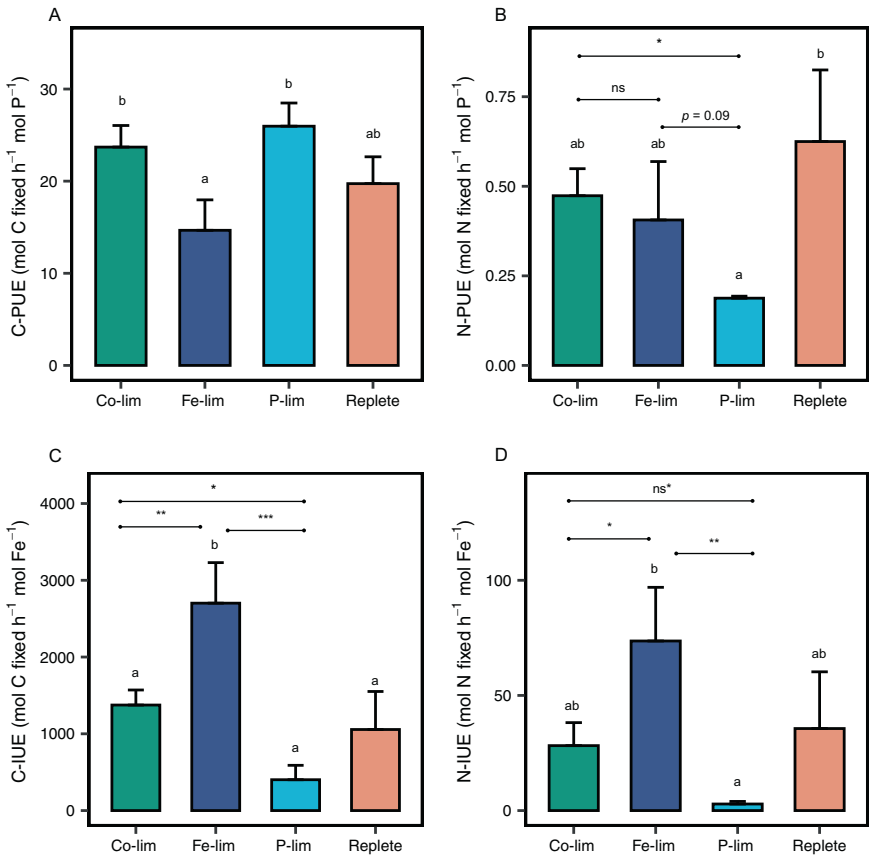

Fig. 2 Calculated elemental use efficiencies (RUEs, mol C or N fixed/hour/mol intracellular P or Fe) of nutrient replete and nutrient-limited *Crocosphaera*. **A** Carbon-specific Phosphorus Use Efficiencies (C-PUEs), **B** Nitrogen-specific Phosphorus Use Efficiencies (N-PUEs), **C** Carbon-specific Iron Use Efficiencies (C-IUEs), and **D** Nitrogen-specific Iron Use Efficiencies (N-IUEs). Error bars denote standard deviation of triplicate values. Different letters on each plot represent statistical significance ($p < 0.05$) calculated by one-way ANOVA across all four treatments. Line segments and corresponding significance markers represent statistical significance calculated by one-way ANOVA across only the nutrient-limited treatments. Plots without line segments indicate that one-way ANOVA results with nutrient-limited only treatments were the same as results calculated with all treatments. Co-lim (Fe/P co-limited, green), Fe-lim (Fe-limited, dark blue), P-lim (P-limited, light blue), and Replete (Fe/P replete, peach). Significance: ns* (no significance, $p > 0.1$ using one-way ANOVA, $p < 0.05$ using Welch's t test), *($p < 0.05$), **($p < 0.01$), ***($p < 0.001$).

for Fe and P-scavenging [15]. However, our study used a relatively low P concentration and had higher biomass than Garcia et al., which may have increased the severity of P limitation in our study and produced smaller cells that were not previously observed.

Cell-normalized C fixation and N_2 fixation rates showed similar patterns across all nutrient treatments (Fig. 1C, D). Replete cells had the highest C fixation and N_2 fixation rates, and Fe-limited cells had the highest rates of the three nutrient-limited treatments. While not statistically significant, co-limited C fixation rates were slightly lower than P-limited rates ($p = 0.085$) and co-limited N_2 fixation rates were ~2 fold higher than P-limited rates ($p > 0.1$).

RUEs can be used as a physiological proxy of enzyme activity and resource allocation by integrating metabolic productivity and resource requirements [27, 46]. Calculated co-limited and P-limited C-PUEs were the highest of the nutrient-limited cells (Fig. 2A, B). Co-limited N-PUEs were comparable to Fe-limited N-PUEs and were more than 2.5-fold higher than P-limited N-PUEs ($p < 0.05$). Fe-limited cells had the highest IUEs while P-limited cells had the lowest (Fig. 2C, D). Co-limited C-IUEs were intermediate of Fe-limited and P-limited cells ($p < 0.01$ and $p < 0.05$, respectively), and although the nutrient-limited one-way ANOVA was not statistically significant ($p = 0.166$), co-limited N-IUEs were ~10 times higher than P-limited N-IUEs ($p < 0.05$ using Welch's unequal variances t test).

We observed similar growth and N_2 fixation rates as Garcia et al. [21] where co-limited cells grew the fastest and exhibited intermediate N_2 fixation rates compared to cells under single-nutrient limitation. Our calculated PUEs and IUEs for P-limited and Fe-limited *Crocosphaera*, respectively, reflect recently published RUEs [46, 67] with the exception of P-limited N-PUEs, which were previously reported to be higher than replete N-PUEs [67] but were observed in our study to be significantly lower. This contrasting N-PUE response could stem from our study using lower P concentrations as well as a large-cell *Crocosphaera* phenotype instead of the small-cell isolate WH8501; the two phenotypes differ in genome size and the number of P acquisition genes [15], possibly leading to varying N-PUEs. Regardless, our P-limited C-PUEs were similar to co-limited C-PUEs, but N-PUEs were lower. Cellular P was comparable between the two treatments (Supplementary Fig. S1), suggesting that P-limited cells may be allocating resources differently compared to other treatments. In particular, high ratios of C fixation to N_2 fixation suggest that P-limited cells favor C fixation compared to cells grown under Fe-limited and co-limited conditions (Supplementary Table S2). This observed nutrient-dependent balance between C and N_2 fixation and elemental ratios (Supplementary Table S3) may have implications for biogeochemical cycling of both major and trace elements across oligotrophic regimes and warrants further study.

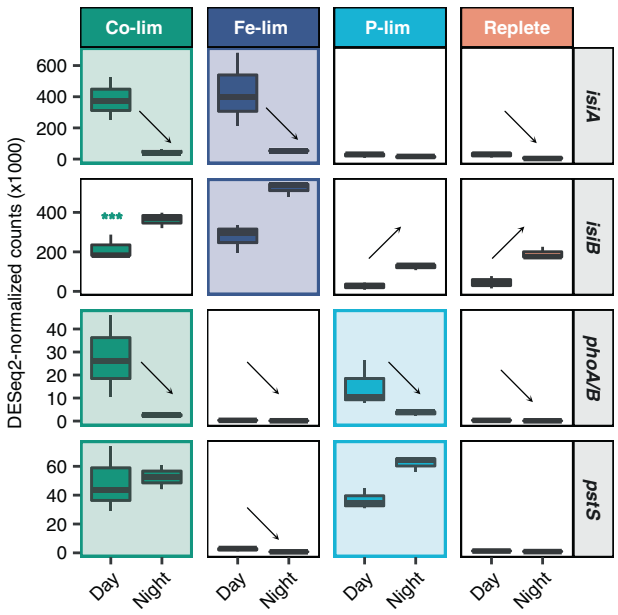

Fig. 3 Gene expression trends of commonly used Fe- and P limitation biomarkers. Statistical significance of biomarkers was calculated from DESeq2 pairwise comparisons of triplicate samples of Co-lim (Fe/P co-limited, green), Fe-lim (Fe-limited, dark blue), P-lim (P-limited, light blue) treatments compared to the Replete (Fe/P replete, peach) treatment. Day and night gene expression significance was calculated from DESeq2 analysis of day and night samples for each nutrient treatment. Shaded-in plots indicate significant upregulation of biomarker genes for both day and night compared to the replete treatment ($p < 0.05$). For the co-limited treatment, only daytime *isiB* gene expression was significantly upregulated compared to the replete treatment at $p < 0.001$ (***). Arrows indicate the directionality of statistically significant trends between day and night gene expression within a treatment ($p < 0.05$).

Crocosphaera diel transcriptome under Fe, P, and Fe/P (co)-limitation

To uncover the mechanisms underlying *Crocosphaera*'s physiological response, we conducted a comparative transcriptomic analysis using DESeq2 on samples collected during peak C fixation (daytime) and N_2 fixation (nighttime). RDA showed samples clustering by nutrient treatment during the day and night (Supplementary Fig. S2A, B) and that sampling time accounts for a large portion of the *Crocosphaera* transcriptomic response (Supplementary Fig. S2C).

We evaluated daytime and nighttime gene expression profiles of commonly used Fe limitation (*isiA*, *isiB*) and P limitation (*phoA/B*, *pstS*) biomarkers to assess cellular nutrient status and found expected gene expression patterns for nutrient-limited cells relative to replete cells (Fig. 3). P limitation genes (*phoA/B* and *pstS*) were upregulated for P-limited and Fe/P co-limited cells, while Fe limitation genes (*isiA* and *isiB*) were upregulated for Fe-limited and co-limited cells. These nutrient biomarkers also exhibited diel trends whereby *isiA* was significantly upregulated during the day for co-limited, Fe-limited, and replete treatments while *isiB* was significantly upregulated at night for P-limited and replete treatments ($p < 0.05$). Nighttime *isiB* expression for Fe-limited and Fe/P co-limited was higher than daytime gene expression, but the difference was not statistically significant ($p = 0.08$ and $p > 0.1$, respectively).

Given the ecological significance of *Crocosphaera* in oligotrophic systems, many studies have sought to identify biomarkers of nutrient limitation that can be used to survey and assess microbial communities in situ [31, 33, 68–70]. Our analyses show that frequently used Fe and P biomarkers can be used to indicate co-limitation in *Crocosphaera*. In addition, previous studies observed diel cycling of *pstS* [32] and *isiB* [14] gene biomarkers in *Crocosphaera*. While our experiment only sampled two-time points, all four biomarkers used in our study showed diel regulation (Fig. 3), affirming that the time of day for sampling and analysis are important considerations when using biomarkers to link nutrient availability, cellular physiology, and ocean biogeochemistry.

Diel regulation of *Crocosphaera*'s transcriptome, especially the temporal separation of photosynthesis and N_2 fixation has been well documented [40, 71–73], with one field study suggesting that nearly half of the transcriptome exhibits a diel pattern [14]. Similarly, our pairwise analysis of day and night gene expression ($p < 0.05$) showed that diel genes accounted for half (51.2%) of *Crocosphaera*'s total transcriptome under replete conditions and demonstrated that nutrient limitation affects diel gene regulation by increasing or decreasing the number of diel genes (Fig. 4A). Fe-limited *Crocosphaera* had the largest diel transcriptome with 58.0 % of genes exhibiting a diel pattern ($n = 2188$) while P-limited *Crocosphaera* had the smallest with 45.8% ($n = 1725$). Co-limited cells fell in between at 55.8% ($n = 2102$).

Genes can be further categorized as "core" genes that are diel across all treatments, "shared" genes upregulated by at least two treatments, and "unique" genes that are diel for only one treatment (Supplementary Fig. S3). A total of 1,018 upregulated core genes (day = 522, night = 496) were identified, comprising more than half of the P-limited (59.0%) and replete (52.7%) diel transcriptomes, but less than half of the co-limited (48.4%) and Fe-limited (46.5%) diel transcriptomes. Co-limited cells had the highest percentage of diel-regulated shared genes and lowest percentage of unique genes which contrasted with P-limited cells.

Overrepresentation analysis identified enriched GO terms and KEGG pathways across core, shared, and unique diel genes (Supplementary Table S4). Core diel genes were enriched in photosynthesis and translation genes for daytime and nighttime, respectively (Fig. 4B). Heatmap visualizations of core GO Biological Process (BP) photosynthesis and translation terms showed that P-limited *Crocosphaera* downregulate both processes compared to other nutrient treatments (Fig. 4C, D, Supplementary Figs. S4, S5A). Hierarchical clustering indicated a similar photosynthesis response for co-limited and Fe-limited cells, while the co-limited translation response resembled P-limited *Crocosphaera*, although P-limited cells have lower gene expression for most of the core genes. While N_2 fixation was not identified through over-representation analysis, the iron protein gene (*nifH*) and molybdenum-iron alpha and beta chain (*nifDK*) nitrogenase genes are core night genes that were significantly upregulated for P-limited cells compared to other nutrient-limited treatments (Supplementary Fig. S6).

Cell division, regulation of cell shape, and peptidoglycan biosynthetic process were also identified as core day GO BP terms with replete and P-limited treatments clustering together and co-limited and Fe-limited clustering together (Supplementary Fig. S5B–D). Fe-limited and co-limited upregulation of cell division, cell shape, and peptidoglycan biosynthesis process correlate with higher growth rates (increased cell division) under Fe limitation and co-limitation compared to P limitation. Upregulation of peptidoglycan biosynthesis may increase the cell's ability to adapt to changing environmental conditions through rearrangement and restructuring of the cell wall [74–77]. Moreover, co-limited and Fe-limited cells shared diel genes for membrane proteins that were constitutively expressed in other treatments (Supplementary Table S4). These results suggest cell wall and membrane flexibility that could benefit Fe-limited and co-limited cells and warrants further study.

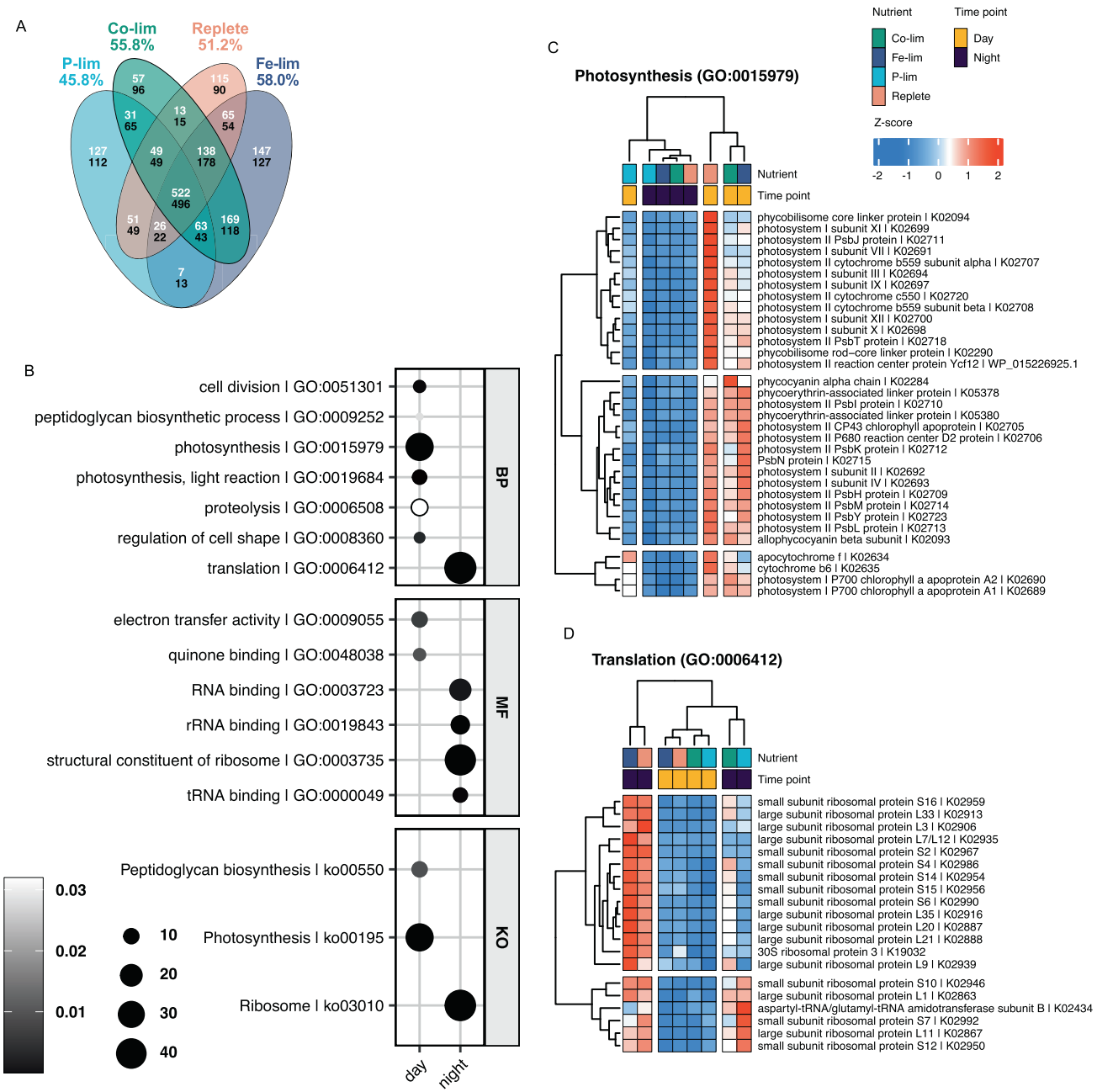

Fig. 4 Diel transcriptomes and core functional enrichment analysis of differentially expressed genes. A Venn Diagram of diel genes for each treatment. The percentages represent the proportion of the overall transcriptome that exhibits a significant diel pattern. The numbers represent the count of genes upregulated during the day (white) and at night (black). **B** Dot plot analysis of enriched GO Biological Process (BP) and Molecular Function (MF) terms and KEGG Pathways (KO) containing diel-regulated genes with p value < 0.05. The size of the dot reflects the number of genes for each term or pathway and the grayscale colorbar reflects the p value. **C** Heatmap analysis showing the DESeq2-normalized gene expression scaled as the number of standard deviations from the row mean (Z-score: red = upregulated, blue = downregulated) for all genes under the Photosynthesis GO term and **D** Heatmap analysis showing the top 25 genes (based on row mean) for the Translation GO term. Due to space constraints, the full Translation heatmap is displayed in the Supplementary Materials (Supplementary Fig. S4). Column dendrograms show similarity based on Euclidean distance and hierarchical clustering and gene clusters were determined by k-means clustering using Euclidean distance. Nutrient treatments are Co-lim (Fe/P co-limited, green), Fe-lim (Fe-limited, dark blue), P-lim (P-limited, light blue), and Replete (Fe/P replete, peach). Time points are Day (goldenrod yellow) and Night (deep purple). The heatmap color gradient shows low gene expression (blue) and high gene expression (red). KEGG annotations were assigned from the genome annotation while non-KEGG annotations were assigned using DIAMOND blastx described in Methods.

Proteolysis genes exhibited a different clustering pattern where the co-limited response clustered more with Fe-limited and replete treatments than with the P-limited treatment (Supplementary Fig. S5E). P-limited cells downregulated a suite of proteolysis genes that were upregulated for Fe-limited and co-limited cells. This includes the *ftsH* gene encoding the FtsH protease responsible for membrane and photosystem protein degradation [78, 79], which hints at a possible disruption of *Crocosphaera*'s diel protein cycling and may explain the differences in diel transcriptomes across the nutrient-limited conditions.

Transcriptomic response of nutrient-limited versus nutrient replete *Crocosphaera*

Pairwise analyses of nutrient-limited treatments (Fe-limited, P-limited, or co-limited) and the replete treatment for day and night (Supplementary Fig. S7A, B) also identified core, shared, and unique DEGs. During the day, the P-limited transcriptome has the most unique DEGs (77.2%) compared to the replete transcriptome. Fe-limited cells had the least with 41.0% as unique genes (Supplementary Fig. S8). At night, P-limited cells also have the largest portion of unique DEGs (68.8%), but co-limited cells have the lowest (29.9%). For both time points, co-limited cells have the largest portion of shared genes, overlapping with both P-limited (36.5%, 30.9%) and Fe-limited (17.0%, 30.8%) treatments for day and night, respectively. Core DEGs comprised a small fraction (i.e., ~2-12%) of the nutrient-limited transcriptomes.

Overrepresentation analysis of unique, upregulated genes indicated that co-limited cells prioritized cell division and regulation of cell shape (GO) and peptidoglycan biosynthesis (KEGG) processes during the day, while P-limited cells upregulated transmembrane transport (GO) and ATP-binding cassette (ABC)-type transporters (KEGG, GO) (Supplementary Fig. S7C). Fe-limited cells were enriched in genes for DNA repair (GO) at night. P-limited cells downregulated genes involved in photosynthesis, transcription, and translation relative to replete cells that were not downregulated by Fe-limited or co-limited cells (Supplementary Fig. S9).

Co- and P-limited cells upregulated shared genes involved in transmembrane transport and downregulated translation (Supplementary Table S5). At night, these cells also upregulated mechanisms that enable their detection and response to environmental stimuli including two-component systems. Simultaneously, co-limited and Fe-limited cells downregulate shared genes predicted to be involved in metal ion binding and iron-sulfur cluster binding.

Linking nutrient-limited diel gene expression to Fe and P-limited physiology

Physiologically, Fe-limited *Crocosphaera* efficiently uses Fe and P for both C and N_2 fixation while P-limited cells are only P-efficient for C fixation and have the lowest RUEs for N_2 fixation. In *Crocosphaera*, low-Fe availability triggers a unique response that moderates P limitation, producing co-limited cells that are more Fe-efficient and highly P-efficient for both C and N_2 fixation, relative to P-limited cells. Core diel genes represent critical cellular functions that maintain a diel pattern regardless of Fe and P availability and constitute a major portion of the diel transcriptome. Thus, differences in gene expression profiles between treatments may contribute to *Crocosphaera*'s observed physiological response to nutrient limitation. Specific nutrient-limited responses can be assessed by looking at the unique and shared DEGs relative to the replete treatment.

Of the nutrient-limited treatments, Fe-limited cells had the highest C and N_2 fixation rates and IUEs likely driven by Fe conservation strategies including recycling Fe between photosynthesis and N_2 fixation pathways [40], replacing ferredoxin with flavodoxin [37], and downregulating PSI genes (Fig. 4C, top cluster) [25]. Of the core diel processes, Fe-limited and replete cells have similar expression profiles for translation genes, suggesting that Fe limitation does not limit ribosomal biogenesis or directly reduce protein synthesis (Fig. 4D, Supplementary Fig. S4). Furthermore, Fe-limited cells (relative to replete cells) uniquely upregulate DNA repair (GO) genes, including *recF*, which is involved in DNA replication and repair (Supplementary Fig. S7C, Supplementary Table S5). Under Fe-limiting conditions, nighttime DNA repair could help offset DNA damage that occurs during photosynthesis-induced cellular oxidative stress [26, 80].

In our study, P-limited cultures were more affected by nutrient limitation than Fe-limited and co-limited cultures, with lower growth and metabolic rates, and RUEs correlating with substantial downregulation of core diel photosynthesis and ribosomal genes that could lead to decreases in cellular function. *Crocosphaera* degrades nitrogenase enzymes during the day and re-synthesizes them de novo at night [14, 40], such that downregulating translation limits their ability to produce nitrogenase proteins and reduces N_2 fixation rates. Accordingly, P-limited *Crocosphaera* had the lowest N_2 fixation rates. Surprisingly though, low rates which suggest low nitrogenase protein abundance corresponded with the highest nighttime *nifHDK* gene counts (Supplementary Fig. S6). Some previous studies have observed that nitrogenase gene expression correlated well with measured N_2 fixation rates [81, 82] while others did not [83, 84]. Regulatory control of N_2 fixation involves transcriptional and post-translational mechanisms that may have decoupled in P-limited cultures [85, 86]. In addition, contrasting P-limited C fixation rates and C-PUEs with N_2 fixation rates and N-PUEs suggest that cells may be allocating more P (e.g., in the form of P-rich ribosomes and ATP) to C fixation. Moreover, functional enrichment suggests that P-limited cells are shifting cellular resources towards building ABC transporters to import nutrients and other growth substrates [87].

Collectively, these responses indicate that P-limited cells may be N/P co-limited, which was evident through additional analyses of N-metabolism biomarkers, cyanophycinase (*cphB*) and the global nitrogen regulator (*ntcA*) (Supplementary Fig. S10). Cyanophycinase (*cphB*) breaks down cyanophycin granules used for N storage and P-limited upregulation of *cphB* during the day and night suggests a need to free up N stores [71, 88, 89]. Additionally, the global nitrogen regulatory gene *ntcA* in cyanobacteria is linked to low N availability and controls the transcription of proteins involved in N assimilation and uptake [68, 90, 91]. In our study, P-limited cells were the only nutrient-limited treatment to significantly upregulate *ntcA* relative to replete cells, suggesting N-limitation stemming from an inability to synthesize nitrogenase proteins at night.

Fe limitation moderates P limitation in a unique Fe/P co-limited phenotype

The combination of Fe limitation and P limitation responses produces a unique Fe/P co-limited *Crocosphaera* phenotype that displays a suite of physiological and molecular characteristics observed in Fe-limited and P-limited cells. A smaller cell size is an important response under nutrient limitation that can reduce nutrient quotas while increasing nutrient uptake. Both co-limited and P-limited cells were comparably small, suggesting P-availability affects cell size.

Previous proteomic analyses of *Trichodesmium* found that while only co-limited cells decreased in size, proteins involved in cell division and size were also abundant for Fe-limited cells, demonstrating that low Fe availability may also exert regulatory control over division and size [44]. In our study, diel transcriptional patterns showed that co-limited and Fe-limited cells similarly upregulated genes for cell division, cell shape, and peptidoglycan biosynthesis, which contribute to cell size [92, 93]. While it is unclear the exact factors regulating *Crocosphaera* cell size flexibility, these results suggest that both Fe and P play an important role.

Altogether, our results suggest that *Crocosphaera* employ two major strategies to manage nutrient limitation: reduction of cellular nutrient requirements and increased responsiveness to environmental change (Fig. 5). Fe limitation in *Crocosphaera* appears to be a strong transcriptional modulator that offsets deleterious effects of P limitation by reducing nutrient requirements through substitution and conservation pathways that were not observed in P-limited cells. P-limited cells primarily increase cellular responsiveness to environmental change (e.g., upregulate two-component regulatory systems) to acquire more P, both inorganic and organic. Fe-limited cells however, prioritize nutrient reduction by substituting out Fe-rich proteins with Fe-free

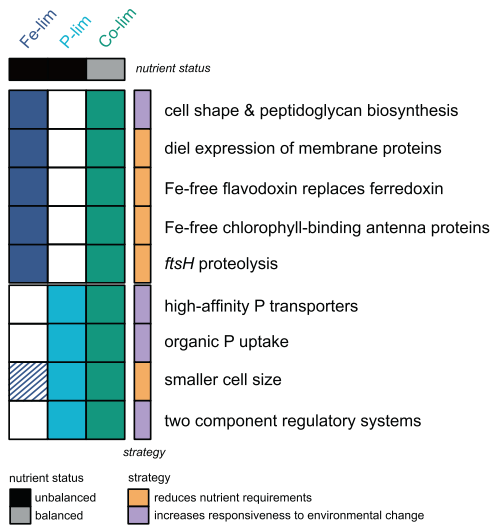

Fig. 5 A schematic of the different strategies and mechanisms to manage single-nutrient limitation (Fe-limited or P-limited) and Fe/P co-limited conditions. For each mechanism, cells that are shaded in represent whether a mechanism is present for a given nutrient-limited treatment and the broad strategy group each mechanism falls under. The partial shading for Fe limitation under the smaller cell size mechanism indicates that while Fe-limited cells were bigger than P-limited and Fe/P co-limited cells, Fe limitation may also play a role in cell size reduction (see the main text for a discussion on *Fe limitation moderates P limitation in a unique Fe/P co-limited phenotype*). Nutrient treatments are Co-lim (Fe/P co-limited, green), Fe-lim (Fe-limited, dark blue), P-lim (P-limited, light blue). Nutrient status is either unbalanced (black) or balanced (gray). Strategy is either reduces nutrient requirements (orange) or increases responsiveness to environmental change (purple).

alternatives, and conserving nutrients, especially N, through diel protein turnover. These single-nutrient limitation mechanisms along with a small cell size manifest simultaneously under Fe/P co-limitation and likely underlie their faster growth rates.

CONCLUSIONS

Our study is among the first to link the physiological and molecular responses of the globally important diazotroph *Crocosphaera* to Fe, P, and Fe/P (co)-limitation, and interpret these relationships in the context of diel gene regulation. The low latitude oceans where N_2 fixers are found are often characterized as being either putatively P-limited or Fe-limited [27, 28]. Our research expands a growing body of work that suggests the reality is more complex than a single nutrient-limited state. The relative availability of nutrients, for example a "balanced" limitation where the normal condition is that both Fe and P are scarce, versus an episodic "imbalanced" state where one nutrient is transitorily available in excess seems to be an important determinant of cellular physiology [43]. We observed a broad metabolic restructuring in *Crocosphaera* in response to P limitation that reduced N_2 fixation and induced cellular N deficiency. In co-limited cells, N deficiency was potentially minimized by the combination of mechanisms upregulated under both P and Fe limitation to produce a unique, comparatively fast-growing and resource-efficient phenotype (Fig. 5). Recent transcriptomic analyses showed that in N-scarce waters, temporal partitioning of N uptake and assimilation enables different microbial groups to coexist [94], suggesting an important regulatory role for N on diel transcription and microbial community structure. In *Crocosphaera*, our analyses showed that Fe and P also exert a regulatory role on diel gene expression. Varying Fe and P availability alter diel gene expression patterns that trigger *Crocosphaera* to dynamically reallocate resources between core cellular processes (e.g., nutrient acquisition, translation, or metabolic rates). These molecular responses underlie unique nutrient-limited physiological responses with implications for the input of new N in oligotrophic systems.

This intersection of N, Fe, and P biogeochemistry reinforces the need to consider differing diazotrophic responses to multiple nutrient limitations. Climate change may alter the existing Fe and P gradient in the ocean. N_2 fixation is projected to shift more towards being P-limited, as intensified stratification reduces advective supplies of P while at the same time, Fe availability increases due to rising anthropogenic aeolian inputs [95, 96]. A better understanding of the nutrient-limited mechanisms and controls of marine N_2 fixation using tools that can capture complex microbial community dynamics (e.g., metatranscriptomics and metaproteomics) will improve our ability to project changes to biogeochemical cycling and primary productivity in a changing ocean.

DATA AVAILABILITY

The physiological data collected from this study are available from BCO-DMO online (http://bcodmo.org). Raw RNAseq reads for differential gene expression analyses are deposited at NCBI's SRA under BioProject PRJNA807802. All scripts to recreate the differential gene expression analyses, statistical analyses, and visualizations are available at https://github.com/yang-nina/CrocosphaeraFePColimitation.

REFERENCES

1. Moore CM, Mills MM, Arrigo KR, Berman-Frank I, Bopp L, Boyd PW, et al. Processes and patterns of oceanic nutrient limitation. Nat Geosci. 2013; https://doi.org/10.1038/ngeo1765.
2. Redfield AC. The biological control of chemical factors in the environment. Am Sci. 1958;46:205–21.
3. Sohm JA, Webb EA, Capone DG. Emerging patterns of marine nitrogen fixation. Nat Rev Microbiol. 2011;9:499–508.
4. Zehr JP, Capone DG. Changing perspectives in marine nitrogen fixation. Science 2020;368:eaay9514.
5. Karl D, Letelier R, Tupas L, Dore J, Christian J, Hebel D. The role of nitrogen fixation in biogeochemical cycling in the subtropical North Pacific Ocean. Nature 1997;388:533–8.
6. Tang W, Cerdán-García E, Berthelot H, Polyviou D, Wang S, Baylay A, et al. New insights into the distributions of nitrogen fixation and diazotrophs revealed by high-resolution sensing and sampling methods. ISME J. 2020;14:2514–26.
7. Tang W, Wang S, Fonseca-Batista D, Dehairs F, Gifford S, Gonzalez AG, et al. Revisiting the distribution of oceanic N_2 fixation and estimating diazotrophic contribution to marine production. Nat Commun. 2019; https://doi.org/10.1038/s41467-019-08640-0.
8. Capone DG, Burns JA, Montoya JP, Subramaniam A, Mahaffey C, Gunderson T, et al. Nitrogen fixation by *Trichodesmium* spp.: an important source of new nitrogen to the tropical and subtropical North Atlantic Ocean. Global Biogeochem Cycles. 2005; https://doi.org/10.1029/2004GB002331.
9. Qu P-P, Fu F-X, Kling JD, Huh M, Wang X, Hutchins DA. Distinct responses of the nitrogen-fixing marine cyanobacterium *Trichodesmium* to a thermally variable environment as a function of phosphorus availability. Front Microbiol. 2019; https://doi.org/10.3389/fmicb.2019.01282.
10. Orchard ED, Webb EA, Dyhrman ST. Molecular analysis of the phosphorus starvation response in *Trichodesmium* spp. Environ Microbiol. 2009;11:2400–11.
11. Capone DG, Zehr JP, Paerl HW, Bergman B, Carpenter EJ. *Trichodesmium*, a globally significant marine cyanobacterium. Science. 1997;276:1221–9.
12. Capone DG, Carpenter EJ. Nitrogen fixation in the marine environment. Science. 1982;217:1140–2.
13. Zehr JP, Waterbury JB, Turner PJ, Montoya JP, Omoregie E, Steward GF, et al. Unicellular cyanobacteria fix N_2 in the subtropical North Pacific Ocean. Nature. 2001;412:635–8.
14. Shi T, Ilikchyan I, Rabouille S, Zehr JP. Genome-wide analysis of diel gene expression in the unicellular N_2-fixing cyanobacterium *Crocosphaera watsonii* WH 8501. ISME J. 2010;4:621–32.
15. Bench SR, Heller P, Frank I, Arciniega M, Shilova IN, Zehr JP. Whole genome comparison of six *Crocosphaera watsonii* strains with differing phenotypes. J Phycol. 2013;49:786–801.
16. Dugenne M, Henderikx Freitas F, Wilson ST, Karl DM, White AE. Life and death of *Crocosphaera* sp. in the Pacific Ocean: Fine scale predator–prey dynamics. Limnol Oceanogr. 2020;65:2603–17.

17. Moisander PH, Beinart RA, Hewson I, White AE, Johnson KS, Carlson CA, et al. Unicellular cyanobacterial distributions broaden the oceanic N_2 fixation domain. Science. 2010;327:1512–4.
18. Detoni AMS, Subramaniam A, Haley ST, Dyhrman ST, Calil PHR. Cyanobacterial diazotroph distributions in the Western South Atlantic. Front Mar Sci. 2022; https://doi.org/10.3389/fmars.2022.856643.
19. Webb EA, Moffett JW, Waterbury JB. Iron stress in open-ocean cyanobacteria (*Synechococcus*, *Trichodesmium*, and *Crocosphaera* spp.): identification of the IdiA protein. Appl Environ Microbiol. 2001; https://doi.org/10.1128/AEM.67.12.5444-5452.2001.
20. Jacq V, Ridame C, L'Helguen S, Kaczmar F, Saliot A. Response of the unicellular diazotrophic cyanobacterium *Crocosphaera watsonii* to iron limitation. PLoS One. 2014;9:e86749.
21. Garcia NS, Fu F, Sedwick PN, Hutchins DA. Iron deficiency increases growth and nitrogen-fixation rates of phosphorus-deficient marine cyanobacteria. ISME J. 2015;9:238–45.
22. Lin S, Litaker RW, Sunda WG. Phosphorus physiological ecology and molecular mechanisms in marine phytoplankton. J Phycol. 2016;52:10–36.
23. Held NA, McIlvin MR, Moran DM, Laub MT, Saito MA. Unique patterns and biogeochemical relevance of two-component sensing in marine bacteria. mSystems. 2019; https://doi.org/10.1128/mSystems.00317-18.
24. Capra EJ, Laub MT. Evolution of two-component signal transduction systems. Annu Rev Microbiol. 2012;66:325–47.
25. Shi T, Sun Y, Falkowski PG. Effects of iron limitation on the expression of metabolic genes in the marine cyanobacterium *Trichodesmium erythraeum* IMS101. Environ Microbiol. 2007;9:2945–56.
26. Schoffman H, Lis H, Shaked Y, Keren N. Iron–nutrient interactions within phytoplankton. Front Plant Sci. 2016; https://doi.org/10.3389/fpls.2016.01223.
27. Hutchins DA, Sañudo-Wilhelmy SA. The enzymology of ocean global change. Ann Rev Mar Sci. 2022;14:187–211.
28. Capone DG. An iron curtain in the Atlantic Ocean forms a biogeochemical divide. Proc Natl Acad Sci USA 2014;111:1231–2.
29. Rouco M, Frischkorn KR, Haley ST, Alexander H, Dyhrman ST. Transcriptional patterns identify resource controls on the diazotroph *Trichodesmium* in the Atlantic and Pacific oceans. ISME J. 2018;12:1486–95.
30. Dyhrman ST, Haley ST. Phosphorus scavenging in the unicellular marine diazotroph *Crocosphaera watsonii*. Appl Environ Microbiol. 2006;72:1452–8.
31. Pereira N, Shilova IN, Zehr JP. Use of the high-affinity phosphate transporter gene, *pstS*, as an indicator for phosphorus stress in the marine diazotroph *Crocosphaera watsonii* (Chroococcales, Cyanobacteria). J Phycol. 2019;55:752–61.
32. Pereira N, Shilova IN, Zehr JP. Molecular markers define progressing stages of phosphorus limitation in the nitrogen-fixing cyanobacterium, *Crocosphaera*. J Phycol. 2016;52:274–82.
33. Frischkorn KR, Haley ST, Dyhrman ST. Transcriptional and proteomic choreography under phosphorus deficiency and re-supply in the N_2 fixing cyanobacterium *Trichodesmium erythraeum*. Front Microbiol. 2019; https://doi.org/10.3389/fmicb.2019.00330.
34. Bibby TS, Nield J, Barber J. Iron deficiency induces the formation of an antenna ring around trimeric photosystem I in cyanobacteria. Nature 2001;412:743–5.
35. Chen HYS, Bandyopadhyay A, Pakrasi HB. Function, regulation and distribution of IsiA, a membrane-bound chlorophyll a-antenna protein in cyanobacteria. Photosynthetica. 2018;56:322–33.
36. Hewson I, Poretsky RS, Beinart RA, White AE, Shi T, Bench SR, et al. In situ transcriptomic analysis of the globally important keystone N_2-fixing taxon *Crocosphaera watsonii*. ISME J. 2009;3:618–31.
37. LaRoche J, Boyd PW, McKay RML, Geider RJ. Flavodoxin as an in situ marker for iron stress in phytoplankton. Nature. 1996;382:802–5.
38. Chappell PD, Webb EA. A molecular assessment of the iron stress response in the two phylogenetic clades of *Trichodesmium*. Environ Microbiol. 2010;12:13–27.
39. Held NA, Waterbury JB, Webb EA, Kellogg RM, McIlvin MR, Jakuba M, et al. Dynamic diel proteome and daytime nitrogenase activity supports buoyancy in the cyanobacterium *Trichodesmium*. Nat Microbiol. 2022;7:300–11.
40. Saito MA, Bertrand EM, Dutkiewicz S, Bulygin VV, Moran DM, Monteiro FM, et al. Iron conservation by reduction of metalloenzyme inventories in the marine diazotroph *Crocosphaera watsonii*. Proc Natl Acad Sci USA 2011;108:2184–9.
41. Mills MM, Ridame C, Davey M, LaRoche J, Geider RJ. Iron and phosphorus co-limit nitrogen fixation in the eastern tropical North Atlantic. Nature. 2004;429:292–4.
42. Held NA, Webb EA, McIlvin MM, Hutchins DA, Cohen NR, Moran DM, et al. Co-occurrence of Fe and P stress in natural populations of the marine diazotroph *Trichodesmium*. Biogeosciences. 2020;17:2537–51.
43. Cérdan-García E, Baylay A, Polyviou D, Woodward EMS, Wrightson L, Mahaffey C, et al. Transcriptional responses of *Trichodesmium* to natural inverse gradients of Fe and P availability. ISME J. 2021; https://doi.org/10.1038/s41396-021-01151-1.
44. Walworth NG, Fu F-X, Webb EA, Saito MA, Moran D, McIlvin MR, et al. Mechanisms of increased *Trichodesmium* fitness under iron and phosphorus co-limitation in the present and future ocean. Nat Commun. 2016; https://doi.org/10.1038/ncomms12081.
45. Price NM, Harrison GI, Hering JG, Hudson RJ, Nirel PMV, Palenik B, et al. Preparation and chemistry of the artificial algal culture medium Aquil. Biol Oceanogr. 1989;6:443–61.
46. Yang N, Merkel CA, Lin Y-A, Levine NM, Hawco NJ, Jiang H-B, et al. Warming iron-limited oceans enhance nitrogen fixation and drive biogeographic specialization of the globally important cyanobacterium *Crocosphaera*. Front Mar Sci. 2021; https://doi.org/10.3389/fmars.2021.628363.
47. Garcia NS, Fu F-X, Breene CL, Yu EK, Bernhardt PW, Mulholland MR, et al. Combined effects of CO_2 and light on large and small isolates of the unicellular N_2-fixing cyanobacterium *Crocosphaera watsonii* from the western tropical Atlantic Ocean. Eur J Phycol. 2013;48:128–39.
48. Jiang H-B, Fu F-X, Rivero-Calle S, Levine NM, Sañudo-Wilhelmy SA, Qu P-P, et al. Ocean warming alleviates iron limitation of marine nitrogen fixation. Nat Clim Chang. 2018;8:709–12.
49. Kustka AB, Sañudo-Wilhelmy SA, Carpenter EJ, Capone D, Burns J, Sunda WG. Iron requirements for dinitrogen- and ammonium-supported growth in cultures of *Trichodesmium* (IMS 101): comparison with nitrogen fixation rates and iron: carbon ratios of field populations. Limnol Oceanogr. 2003;48:1869–84.
50. Hawco NJ, Fu F, Yang N, Hutchins DA, John SG. Independent iron and light limitation in a low-light-adapted *Prochlorococcus* from the deep chlorophyll maximum. ISME J. 2020;15:359–62.
51. Andrews S. FastQC: a quality control tool for high throughput sequence data. 2010.
52. Bolger AM, Lohse M, Usadel B. Trimmomatic: a flexible trimmer for Illumina sequence data. Bioinformatics. 2014;30:2114–20.
53. Qu P-P, Fu F-X, Wang X-W, Kling JD, Elghazzawy M, Huh M, et al. Two co-dominant nitrogen-fixing cyanobacteria demonstrate distinct acclimation and adaptation responses to cope with ocean warming. Environ Microbiol Rep. 2022; https://doi.org/10.1111/1758-2229.13041.
54. Langmead B, Salzberg SL. Fast gapped-read alignment with Bowtie 2. Nat Methods. 2012;9:357–9.
55. Li H, Handsaker B, Wysoker A, Fennell T, Ruan J, Homer N, et al. The Sequence alignment/map format and SAMtools. Bioinformatics. 2009;25:2078–9.
56. Liao Y, Smyth GK, Shi W. featureCounts: an efficient general purpose program for assigning sequence reads to genomic features. Bioinformatics. 2014;30:923–30.
57. Kanehisa M, Goto S. KEGG: Kyoto encyclopedia of genes and genomes. Nucleic Acids Res. 2000;28:27–30.
58. Leonhardt K, Straus NA. An iron stress operon involved in photosynthetic electron transport in the marine cyanobacterium *Synechococcus* sp. PCC 7002. J Gen Microbiol. 1992;138:1613–21.
59. Love MI, Huber W, Anders S. Moderated estimation of fold change and dispersion for RNA-seq data with DESeq2. Genome Biol. 2014; https://doi.org/10.1186/s13059-014-0550-8.
60. Yu G, Wang L-G, Han Y, He Q-Y. clusterProfiler: an R package for comparing biological themes among gene clusters. OMICS. 2012;16:284–7.
61. Buchfink B, Reuter K, Drost H-G. Sensitive protein alignments at tree-of-life scale using DIAMOND. Nat Methods. 2021;18:366–8.
62. Conesa A, Götz S, García-Gómez JM, Terol J, Talón M, Robles M. Blast2GO: a universal tool for annotation, visualization and analysis in functional genomics research. Bioinformatics. 2005;21:3674–6.
63. Chille E, Strand E, Neder M, Schmidt V, Sherman M, Mass T, et al. Developmental series of gene expression clarifies maternal mRNA provisioning and maternal-to-zygotic transition in a reef-building coral. BMC Genom. 2021; https://doi.org/10.1186/s12864-021-08114-y.
64. Jones P, Binns D, Chang H-Y, Fraser M, Li W, McAnulla C, et al. InterProScan 5: genome-scale protein function classification. Bioinformatics. 2014;30:1236–40.
65. Oksanen J, Guillaume Blanchet F, Friendly M, Kindt R, Legendre P, McGlinn D, et al. vegan: Community Ecology Package. R package version 2.5-7. 2020.
66. Finkel ZV, Beardall J, Flynn KJ, Quigg A, Rees TAV, Raven JA. Phytoplankton in a changing world: cell size and elemental stoichiometry. J Plankton Res. 2010;32:119–37.
67. Deng L, Cheung S, Kang C-K, Liu K, Xia X, Liu H. Elevated temperature relieves phosphorus limitation of marine unicellular diazotrophic cyanobacteria. Limnol Oceanogr. 2021; https://doi.org/10.1002/lno.11980.
68. Saito MA, McIlvin MR, Moran DM, Goepfert TJ, DiTullio GR, Post AF, et al. Multiple nutrient stresses at intersecting Pacific Ocean biomes detected by protein biomarkers. Science. 2014;345:1173–7.
69. Walworth NG, Saito MA, Lee MD, McIlvin MR, Moran DM, Kellogg RM, et al. Why environmental biomarkers work: Transcriptome-proteome correlations and modeling of multistressor experiments in the marine bacterium *Trichodesmium*. J Proteome Res. 2021; https://doi.org/10.1021/acs.jproteome.1c00517.
70. Hook SE, Gallagher EP, Batley GE. The role of biomarkers in the assessment of aquatic ecosystem health. Integr Environ Assess Manag. 2014;10:327–41.

71. Dron A, Rabouille S, Claquin P, Le Roy B, Talec A, Sciandra A. Light-dark (12:12) cycle of carbon and nitrogen metabolism in *Crocosphaera watsonii* WH8501: relation to the cell cycle. Environ Microbiol. 2012;14:967–81.
72. Mohr W, Intermaggio MP, LaRoche J. Diel rhythm of nitrogen and carbon metabolism in the unicellular, diazotrophic cyanobacterium *Crocosphaera watsonii* WH8501. Environ Microbiol. 2010;12:412–21.
73. Wilson ST, Aylward FO, Ribalet F, Barone B, Casey JR, Connell PE, et al. Coordinated regulation of growth, activity and transcription in natural populations of the unicellular nitrogen-fixing cyanobacterium *Crocosphaera*. Nat Microbiol. 2017;2:9.
74. Silhavy TJ, Kahne D, Walker S. The bacterial cell envelope. *Cold Spring Harb Perspect Biol*. 2010; https://doi.org/10.1101/cshperspect.a000414.
75. Scheffers D-J, Pinho MG. Bacterial cell wall synthesis: new insights from localization studies. Microbiol Mol Biol Rev. 2005;69:585–607.
76. Cava F, de Pedro MA. Peptidoglycan plasticity in bacteria: emerging variability of the murein sacculus and their associated biological functions. Curr Opin Microbiol. 2014;18:46–53.
77. Mueller EA, Levin PA. Bacterial cell wall quality control during environmental stress. mBio. 2020; https://doi.org/10.1128/mBio.02456-20.
78. Langklotz S, Baumann U, Narberhaus F. Structure and function of the bacterial AAA protease FtsH. Biochim Biophys Acta. 2012;1823:40–48.
79. Bonisteel EM, Turner BE, Murphy CD, Melanson J-R, Duff NM, Beardsall BD, et al. Strain specific differences in rates of Photosystem II repair in picocyanobacteria correlate to differences in FtsH protein levels and isoform expression patterns. PLoS One. 2018;13:e0209115.
80. Latifi A, Ruiz M, Zhang C-C. Oxidative stress in cyanobacteria. FEMS Microbiol Rev. 2009;33:258–78.
81. Zehr JP, Montoya JP, Jenkins BD, Hewson I, Mondragon E, Short CM, et al. Experiments linking nitrogenase gene expression to nitrogen fixation in the North Pacific subtropical gyre. Limnol Oceanogr. 2007;52:169–83.
82. Benavides M, Duhamel S, Van Wambeke F, Shoemaker KM, Moisander PH, Salamon E, et al. Dissolved organic matter stimulates N_2 fixation and *nifH* gene expression in *Trichodesmium*. FEMS Microbiol Lett. 2020; https://doi.org/10.1093/femsle/fnaa034.
83. Turk-Kubo KA, Achilles KM, Serros TRC, Ochiai M, Montoya JP, Zehr JP. Nitrogenase (*nifH*) gene expression in diazotrophic cyanobacteria in the Tropical North Atlantic in response to nutrient amendments. Front Microbiol. 2012; https://doi.org/10.3389/fmicb.2012.00386.
84. Turk KA, Rees AP, Zehr JP, Pereira N, Swift P, Shelley R, et al. Nitrogen fixation and nitrogenase (*nifH*) expression in tropical waters of the eastern North Atlantic. ISME J. 2011;5:1201–12.
85. Zehr JP, Wyman M, Miller V, Duguay L, Capone DG. Modification of the Fe protein of nitrogenase in natural populations of *Trichodesmium thiebautii*. Appl Environ Microbiol. 1993;59:669–76.
86. Dixon R, Kahn D. Genetic regulation of biological nitrogen fixation. Nat Rev Microbiol. 2004;2:621–31.
87. Tang K, Jiao N, Liu K, Zhang Y, Li S. Distribution and functions of TonB-dependent transporters in marine bacteria and environments: implications for dissolved organic matter utilization. PLoS One. 2012;7:e41204.
88. Finzi-Hart JA, Pett-Ridge J, Weber PK, Popa R, Fallon SJ, Gunderson T, et al. Fixation and fate of C and N in the cyanobacterium *Trichodesmium* using nanometer-scale secondary ion mass spectrometry. Proc Natl Acad Sci USA 2009;106:6345–50.
89. Watzer B, Forchhammer K. Cyanophycin synthesis optimizes nitrogen utilization in the unicellular cyanobacterium *Synechocystis* sp. strain PCC 6803. Appl Environ Microbiol. 2018; https://doi.org/10.1128/AEM.01298-18.
90. Lindell D, Padan E, Post AF. Regulation of ntcA expression and nitrite uptake in the marine *Synechococcus* sp. strain WH 7803. J Bacteriol. 1998;180:1878–86.
91. Tolonen AC, Aach J, Lindell D, Johnson ZI, Rector T, Steen R, et al. Global gene expression of *Prochlorococcus* ecotypes in response to changes in nitrogen availability. Mol Syst Biol. 2006; https://doi.org/10.1038/msb4100087.
92. Si F, Le Treut G, Sauls JT, Vadia S, Levin PA, Jun S. Mechanistic origin of cell-size control and homeostasis in bacteria. Curr Biol. 2019; https://doi.org/10.1016/j.cub.2019.04.062.
93. Chien A-C, Hill NS, Levin PA. Cell size control in bacteria. Curr Biol. 2012; https://doi.org/10.1016/j.cub.2012.02.032.
94. Muratore D, Boysen AK, Harke MJ, Becker KW, Casey JR, Coesel SN, et al. Complex marine microbial communities partition metabolism of scarce resources over the diel cycle. Nat Ecol Evol. 2022;6:218–29.
95. Hutchins DA, Boyd PW. Marine phytoplankton and the changing ocean iron cycle. Nat Clim Chang. 2016; https://doi.org/10.1038/nclimate3147.
96. Hutchins DA, Capone DG. The marine nitrogen cycle: new developments and global change. Nat Rev Microbiol. 2022;20:401–14.

ACKNOWLEDGEMENTS

This research was supported by U.S. National Science Foundation Biological Oceanography program grants OCE 1657757, OCE 1851222 to DAH, FXF, and EAW, OCE 2149837 to DAH and FXF, SCOR Working Group 149, as well as graduate student support from a USC Provost Fellowship to NY. We would also like to thank three anonymous reviewers who provided comments to improve this manuscript.

AUTHOR CONTRIBUTIONS

NY, F-FX, P-PQ, and DAH designed the experiment. NY carried out the experiment, with significant support from Y-AL, CAM, and MAD in monitoring cultures using cell-based growth rates and experimental maintenance. P-PQ and F-XF also contributed to experimental maintenance and support with physiological data analysis. NY collected large-volume samples, extracted RNA for transcriptomics analyses, and conducted differential gene expression analyses with support from P-PQ and EAW. NY wrote the manuscript with input from EAW and DAH. All authors reviewed and gave their approval for the final manuscript.

COMPETING INTERESTS

The authors declare no competing interests.

ADDITIONAL INFORMATION

Supplementary information The online version contains supplementary material available at https://doi.org/10.1038/s41396-022-01307-7.

Correspondence and requests for materials should be addressed to David A. Hutchins.